Comparative Study of Photoswitchable Zinc-Finger Domain and AT-Hook Motif for Light-Controlled Peptide-DNA Binding

Murawska, Gosia M.; Poloni, Claudia; Simeth, Nadja A.; Szymanski, Wiktor; Feringa, Ben L.

Published in:
Chemistry

DOI:
10.1002/chem.201900090

Publication date:
2019

FULL PAPER

Comparative study of photoswitchable zinc finger domain and AT-hook motif for light-controlled peptide-DNA binding

Gosia M. Murawska,[a] Claudia Poloni,[a] Nadja A. Simeth,[a] Wiktor Szymanski[a,b],* and Ben L. Feringa [a],*

Abstract: DNA-peptide interactions are involved in key life processes, including DNA recognition, replication, transcription, repair, organization and modification. Development of tools that can influence DNA-peptide binding non-invasively with high spatiotemporal precision could aid in determining its role in cells and tissues. Here, we report on the design, synthesis and study of photocontrolled tools for sequence-specific small peptide-DNA major and minor groove interactions, shedding light on DNA binding by transcriptionally active peptides. In particular, photoswitchable moieties were implemented in the peptide backbone or turn region. In each case, DNA binding was affected by photochemical isomerization, as determined in fluorescent displacement assays on model DNA strands, which provides promising tools for DNA modulation.

Introduction

Peptide–DNA interactions are abundant in the living cell and increased understanding of these interactions has provided important insight into various molecular signaling pathways.[1] To offer the potential to obtain external control over gene expression, various parameters to influence molecular interactions in biological systems were considered, including temperature, metal and ligand interactions, pH and ionic strength.[2] However, such manipulations often lead to unwanted side effects and cannot be delivered with high spatiotemporal precision *in vivo*.[3] These limitations might be overcome by the use of light as a bioorthogonal external trigger. Unlike methods currently used to modulate peptide-DNA interactions, light can be applied to specific areas with high resolution causing minimal to no perturbation to biological systems.[4]

Light-driven control over DNA–peptide interactions can be achieved by using molecular photoswitches.[4a-c] These compounds have two or more stable isomeric forms that can be interconverted with light, and include azobenzenes,[5] diarylethenes[6] and stilbenes, amongst others.[7] Especially, azobenzenes are widely used as switching elements in biological[5a] and bioorthogonal systems,[5b] due to their relatively easy synthesis, a strongly pronounced difference in shape and polarity between the isomers and favorable photochemical properties, including fatigue resistance and high switching amplitude.[4a-c, 5, 8] Thereby, the *E*-form of azobenzenes can be isomerized into its *Z*-form applying UV light irradiation (*cf.* Figure 1A for an azobenzene derivative). The process can be reversed using visible light or through thermal relaxation.[6b, 9]

Azobenzene moieties have been employed to modulate peptide-DNA binding.[4a-c, 4e, 5a, 10] These efforts have enabled photo-responsive DNA-azobenzene self-assembly for photo-controlled drug delivery[11] and DNA compaction.[12] Commonly, Azobenzene-modified peptidic DNA-binders are designed such that an azobenzene moiety is incorporated within or appended to the structure of a preexisting peptidic DNA-binder. This permits the use of light for control over the peptide structure, thereby influencing its binding affinity for its DNA target.[4a, b, 5a, 13] In this work, we focus on two main classes of peptide-DNA binders; major groove and minor groove binders (Figure 1B). The first group includes proteins that bind to DNA via α-helical domains,[14] such as leucine zipper domains,[15] and β-hairpin structures, such as β-turn and β-strand motifs.[16] When designing photocontrollable α-helix structures, the photoswitchable moieties can be used to substitute amino acids in the backbone or as cross-linkers between two side chains.[8c, 17] For β-turn structures, the azobenzene unit is generally inserted into the turn region of a peptide.[18] The second group, the minor groove binders, mainly comprises oligopeptides that interact with DNA *via* electrostatic interactions.[19] To the best of our knowledge, there are so far no examples of photoswitchable peptides that bind to the DNA minor groove.

Our photocontrolled minor groove binder was designed based on the AT-Hook binding motif from the A1 group of the High Mobility Group (HMG) protein family (Figure 1C). These proteins have been implicated in cancer growth and propagation and are therefore important targets to study tumorigenesis. The conserved, palindromic core binding sequence Arginine-Glycine-Arginine (RGR) is supposed to be crucial for interaction of the protein to adenine-thymine (AT)-rich DNA minor grooves.[20] Hence, we aimed to combine the RGR-motif with azobenzene to develop a photoswitchable minor groove binder.

As a major groove-binder, we chose the zinc finger domain.[21] In general, zinc fingers represent the binding elements of transcription factors and bind to DNA *via* at least three units.[21a] Thus, they play an important role in gene expression. The domain consists of two β-strands and one DNA-binding α-helix motif. The coordination of a zinc ion (Zn^{2+}) stabilizes the peptide's tertiary structure (Figure 1D),[22] which we intended to control photochemically in the present study for the first time. In previous approaches regarding the photocontrol of peptidic DNA-binders using a zinc finger-bearing protein, the photoresponsive unit did not influence the tertiary structure of the zinc finger domain. For instance, the group or Deiters caged the biological activity with a photolabile protecting group.[23] Okamoto and co-workers appended the photoswitch onto the *N*-terminus, close to the α-helix, which influences the accessibility to the DNA binding site rather than the protein's structure.[24] Conversely, we focused our

[a] G. M. Murawska, Dr. C. Poloni, Dr. N. A. Simeth, Dr. W. Szymanski, Prof. Dr. B. L. Feringa
Centre for Systems Chemistry, Stratingh Institute for Chemistry
University of Groningen
Nijenborgh 4, 9747 AG Groningen (The Netherlands)
E-mail: b.l.feringa@rug.nl

[b] Dr. W. Szymanski
Department of Radiology
University of Groningen, University Medical Centre Groningen
Hanzeplein 1, 9713 GZ Groningen (The Netherlands)
E-mail: w.szymanski@umcg.nl

Supporting information for this article is given via a link at the end of the document.

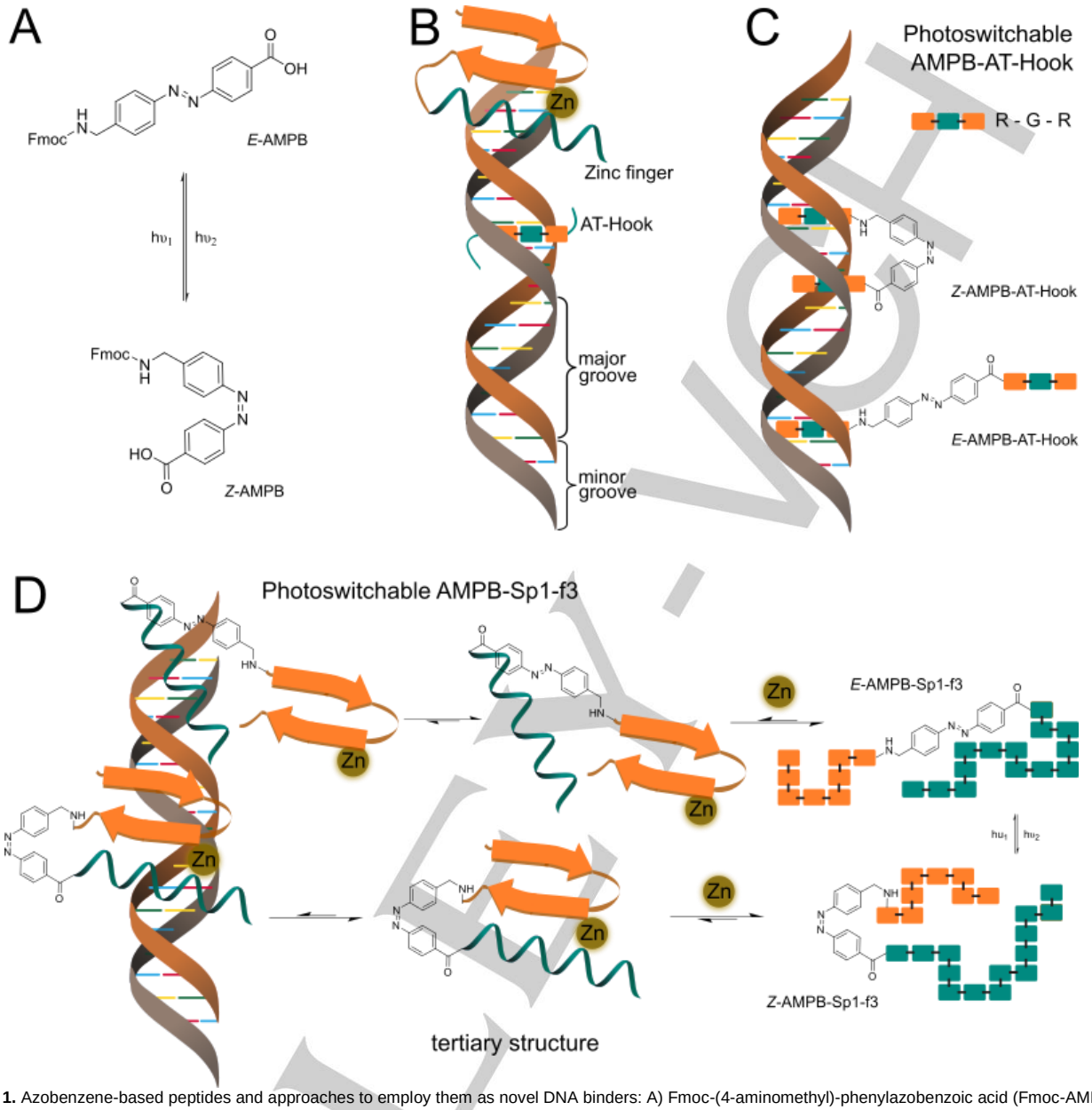

Figure 1. Azobenzene-based peptides and approaches to employ them as novel DNA binders: A) Fmoc-(4-aminomethyl)-phenylazobenzoic acid (Fmoc-AMPB) in its thermodynamically stable *E*- and metastable *Z*-form. Their interconversion can be triggered through irradiation with 365 nm (*E*→*Z*) or white light (*Z*→*E*), respectively. B) Schematic representation of the zinc finger Sp1-f3 and the AT-Hook binding motif from the A1 group of the High Mobility Group (HMG) protein family at their respective binding site at a DNA strand. C) Design principle of a photoswitchable AT-Hook as presented in this study. The *E*-isomer should only be able to intercalate with one RGR-motif, whereas the *Z*-isomer should be able to bind with two RGR-units at the same DNA strand. D) Design of a photoswitchable zinc finger bearing the azo-unit in the backbone of the peptide chain. The folding of the peptide should occur after addition of Zn^{2+} in both photoisomers. However, formation of a functional tertiary structure should be more disrupted in the *E*-form of the switch than in the *Z*-isomer.

efforts on developing a system in which the photoswitchable unit interferes with the Zn^{2+}- mediated folding into the tertiary structure of a single Zn^{2+}- binding module, thereby influencing major groove binding (Figure 1D), rather than on developing a binder with high affinity, such as native zinc finger with several binding modules. In this manner, specific photoswitchable major and minor groove binders were developed and investigated regarding their photochromic properties and their DNA-binding proficiency using fluorescence displacements assays.

Results and Discussion

Design. Our design of both photoresponsive DNA-binders is based on the incorporation of an azobenzene switch into the peptide backbone. To facilitate this, we used (4-aminomethyl)phenylazobenzoic acid (AMPB, Figure 1A), a switch that can be employed in solid phase peptide synthesis (SPPS), as previously reported by Chmielewski and co-workers.[25] To obtain a photoswitchable AT-Hook, we positioned AMPB between two RGR-functions (Figure 1C and 2A). Being attached on opposite sides of the switch, only one RGR-moiety should be able to bind to the minor groove of the (same) DNA strand in the *E*-isomer. However, the geometry of the *Z*-isomer should allow both core binding motifs to interact with the DNA strand and

consequently result in a stronger binding affinity (Figure 1C). A related approach has been reported with a peptide-conjugated, light-driven molecular motor.[26]

In the case of the zinc finger, the azobenzene was incorporated into the turn region of the mammalian factor Sp1 to separate the β1/β2 from the α-helix sequences (Figure 2B).[27] We expected that the structure of the peptide would be disrupted to a larger extent in the *E*-isomer of the switch than in the *Z*-form. Hence, binding of Zn^{2+} and folding into the tertiary structure of the zinc finger domain should differ and, ultimately, the affinity of the peptide towards the DNA helix should be influenced by the photoisomer present (Figure 1D). We envisioned that the introduction of a photochromic function in this crucial position can represent a general approach to develop photoswitchable zinc fingers.

Synthesis. The azobenzene building block Fmoc-AMPB-OH was synthesized following published protocols[25, 28] and employed to obtain both the AMPB-Sp1-f3 and the AMPB-AT-Hook *via* SPPS (Figure 2).[29] However, applying standard amino acid side chain deprotection strategies using silanes as cation scavengers resulted in the reduction of the diazo moiety of the photoswitch.[30] Therefore, we instead used a solution of a 95:5 TFA-water mixture. After cleavage from the resin and removal of the side-chain protecting groups, the crude peptides were purified through preparative HPLC and their identities were confirmed by MALDI-TOF mass analysis (see Supporting Information). In addition, we synthesized the natural Sp1-f3 peptide (Figure 1B) as a reference compound for DNA binding studies (*vide infra*).

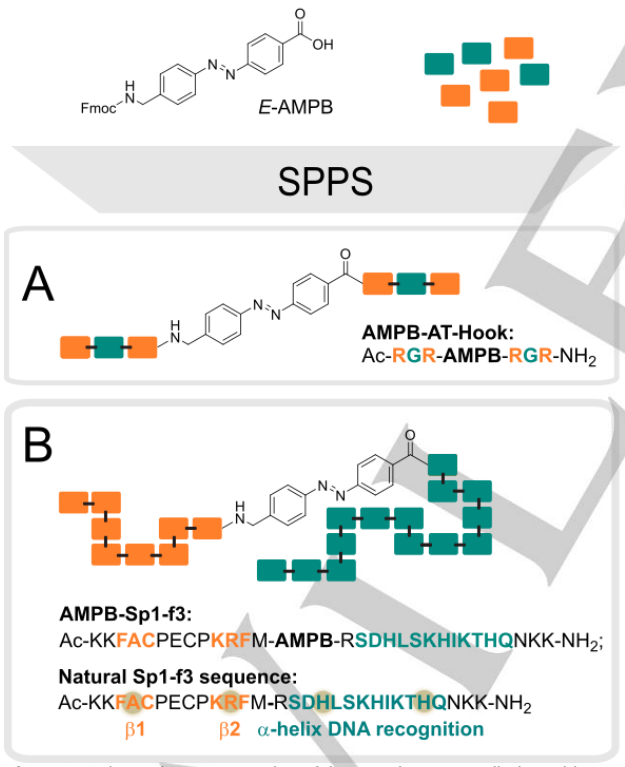

Figure 2. Schematic representation of the two photo-controlled peptides. Using Fmoc-AMPB-OH as building block in SPPS,[25] AMPB-AT-Hook (A, sequence depicted) and AMPB-Sp1-f3 (sequence depicted) were obtained. AMPB-Sp1-f3 was derived from the natural Sp1-f3 peptide (sequence shown in B, the amino acids involved in the binding of Zn^{2+} in Sp1-f3) are highlighted.[27]

Photochemical Characterization. Both AMPB-containing peptides were analyzed by UV-vis spectroscopy and analytical HPLC. The absorption spectra of AMPB-Sp1-f3 in DMSO/MeOH (1:9) and AMPB-AT-Hook in water are depicted in Figure 3A and 3B, respectively. In both cases, the *E*-isomer exhibits a main transition band at λ_{max} = 332 nm (π–π* transition). Upon irradiation with λ_{irrad} = 365 nm, this band decreases, which is accompanied by formation of a low intensity band at λ_{max} = 435 nm (AMPB-Sp1-f3) or 429 nm (AMPB-AT-Hook) which can be attributed to the n–π* transition of the newly formed *Z*-isomer.[15d, e] The photostationary distribution (PSD) was assigned in aqueous buffer to be at least 44:56 (AMPB-Sp1-f3) or 33:67 (AMPB-AT-Hook; *E*:*Z* ratio) at the photostationary state ($PSS_{E\rightarrow Z}$) using analytical HPLC (*cf.* Supporting Information). Isosbestic points at λ_{iso} = 286 nm and 391 nm, or at 239 nm, 286 nm and 394 nm, respectively, indicate a clear two-component photoswitching process (Figure 3). Through irradiation of the solution at the $PSS_{E\rightarrow Z}$ with white light, the photoisomerization can be reverted, accumulating the *E*-form in the resulting $PSS_{Z\rightarrow E}$ (olive line, Figure 3A). Both AMPB-Sp1-f3 and AMPB-AT-Hook are stable over at least three switching cycles (inserted in Figure 3A and B).

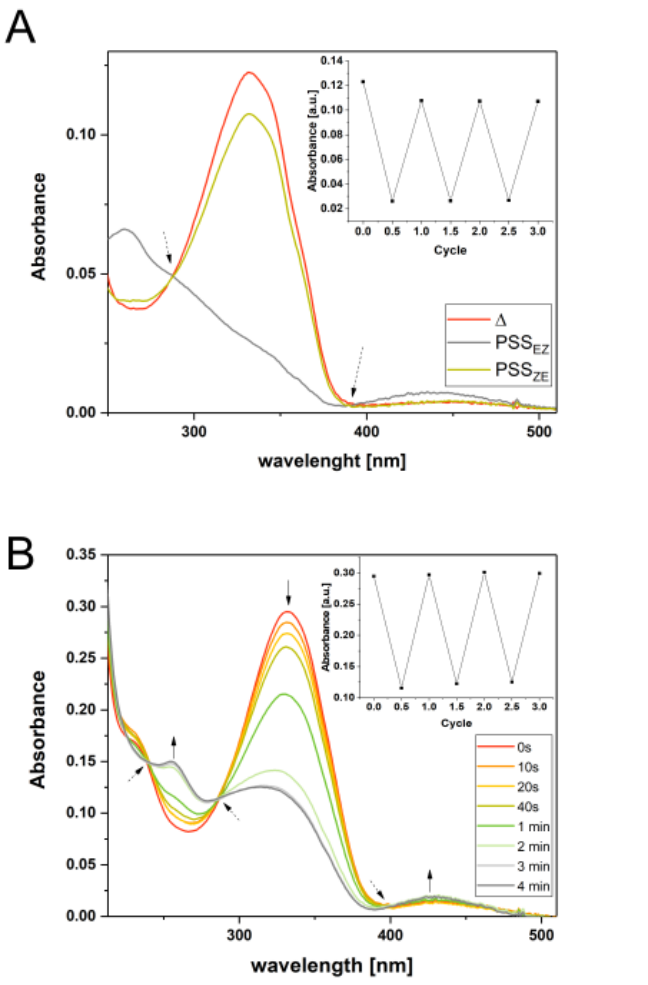

Figure 3. Photochromic properties of the photoswitchable peptides presented in this work. A) UV-vis spectrum of AMPB-Sp1-f3 in DMSO/MeOH (1:9) at the thermal equilibrium (red), the $PSS_{E\rightarrow Z}$ (gray) and the $PSS_{Z\rightarrow E}$ (olive). Dashed arrows indicate isosbestic points. The insert shows repeated UV/white light irradiation cycles. B) UV-vis spectrum of AMPB-AT-Hook in water. The stepwise irradiation with light of 365 nm induces isomerization from the *E*-isomer (red line) to the $PSS_{E\rightarrow Z}$ (gray line), which mainly contains the *Z*-isomer and the $PSS_{Z\rightarrow E}$ (yellow). Dashed arrows indicate isosbestic points. The insert shows repeated UV/white light irradiation cycles.

The thermal stability of the *Z*-isomers in aqueous buffer was investigated by following the recovery of the absorbance at λ_{max} = 332 nm from the $PSS_{E\rightarrow Z}$ in the dark (Supporting Information). In case of AMPB-Sp1-f3, the experiment was conducted in both the presence and absence of Zn^{2+} (one equiv. with respect to AMPB-Sp1-f3), to verify whether the zinc binding influences the thermal half-life of the azobenzene-peptide. All compounds exhibit thermal half-lives in the hour-range in TRIS buffer (see Supporting Information for details). Furthermore, the half-life of Zn^{2+}-bound AMPB-Sp1-f3 is significantly longer than without metal ($\tau_{1/2}$ = 36 h or 14 h, respectively). Since the coordination of zinc is crucial for the formation of the functional tertiary structure,[8c, 17] we attribute this increased stability of the *Z*-isomer to an improved folding of the peptide. Moreover, the AMPB-AT-Hook exhibits the thermally most stable *Z*-isomer as we could observe hardly any *Z*-to-*E* isomerization over more than 50 h (*cf.* Supporting Information).

CD spectroscopy. Additional analyses of AMPB-Sp1-f3 were performed using CD spectroscopy in order to study the influence of irradiation and the presence of Zn^{2+} on the formation of the tertiary structure of the peptide.[22] Thereby, native Sp1-f3 was used as a reference. In particular, apo-Sp1-f3 exhibits strongly negative molar ellipticity at λ = 200 nm and a weaker but broader CD band around λ = 230 nm (Figure 4A). Addition of Zn^{2+} leads to changes in the CD spectrum:[22] in accordance with folding into the tertiary structure of the zinc finger and previous reports, the negative molar ellipticity at λ = 200 nm is reduced and slightly shifted to λ = 205 nm. In addition, the broad band around λ = 230 nm is sharpening and becoming more intense (λ = 226 nm, Figure 4A).[22] Next, we analyzed the CD spectrum of AMPB-Sp1-f3 in the presence and absence of Zn^{2+} and the influence of photoswitching by irradiation with light (Figure 4B and Supporting Information). Similar to native Sp1-f3, the photoswitch shows both in the thermally stable *E*-isomer and at the $PSS_{E\rightarrow Z}$ (containing the *Z*-isomer) strongly negative molar ellipticity around λ = 200 nm and a less intense, but broader band around λ = 230 nm. In our design, we anticipated that the *Z*-isomer should geometrically favor binding of Zn^{2+} and hence, favor proper folding of the protein (*cf.* Figure 1D). Consequently, we added one equivalent of Zn^{2+} to AMPB-Sp1-f3 at the $PSS_{E\rightarrow Z}$ (to result in $^{Zn}PSS_{E\rightarrow Z}$) and followed binding by CD spectroscopy. Figure 4B shows that the negative molar ellipticity at λ = 200 nm is reduced and, similarly as in the native Sp1-f3, shifted to λ = 205 nm indicating a Zn^{2+}-mediated folding taking place. In contrast to the native Sp1-f3, the broad band around λ = 230 nm appears to be not influenced. Another indication for Zn^{2+} binding towards AMPB-Sp1-f3 can be found in the UV-vis spectrum (Figure 4D).

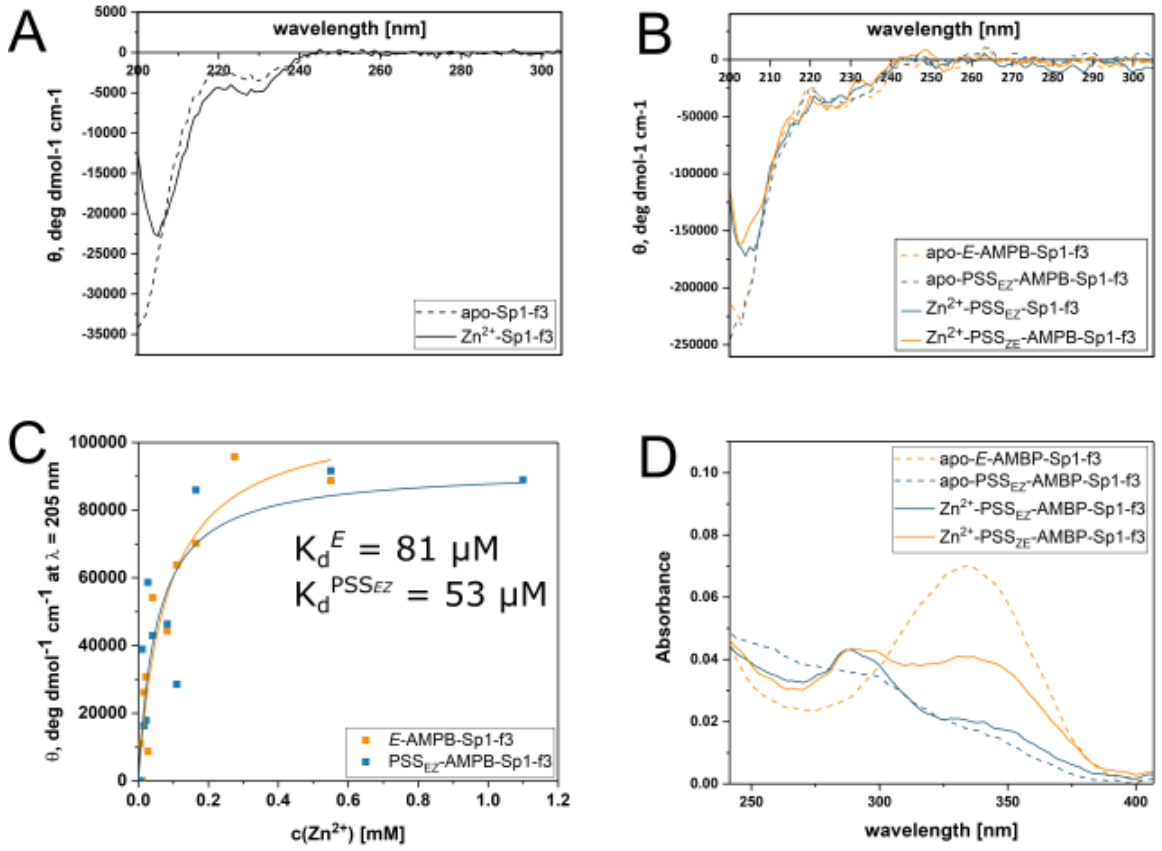

Figure 4. Folding into the tertiary structure of (photoswitchable) zinc finger can be followed by CD and UV-vis spectroscopy. A) CD spectrum of native Sp1-f3 without (dashed line) and with (solid line) Zn^{2+} addition. B) CD spectrum of AMPB-Sp1-f3 at the thermal equilibrium (dashed orange line) and the $PSS_{E\rightarrow Z}$ (blue dashed line) without Zn^{2+}. After addition of the $ZnCl_2$ solution at the $PSS_{E\rightarrow Z}$ (blue solid line) the molar ellipticity at 200 nm deceases in intensity. Furthermore, switching to the $^{Zn}PSS_{Z\rightarrow E}$ (orange solid line) did not result in significant changes. C) By titrating Zn^{2+} to solutions of AMPB-Sp1-f3 at the thermodynamic equilibrium (orange line) and at the $PSS_{E\rightarrow Z}$ (blue line) the affinity towards the Zn^{2+} ion could be determined. D) UV-vis spectrum of apo-AMPB-Sp1-f3 at the thermal equilibrium (dashed orange line) and the $PSS_{E\rightarrow Z}$ (blue dashed line). Through addition of Zn^{2+} an additionally transition band at 288 nm becomes visible and is also present at the $^{Zn}PSS_{Z\rightarrow E}$ (orange solid line).

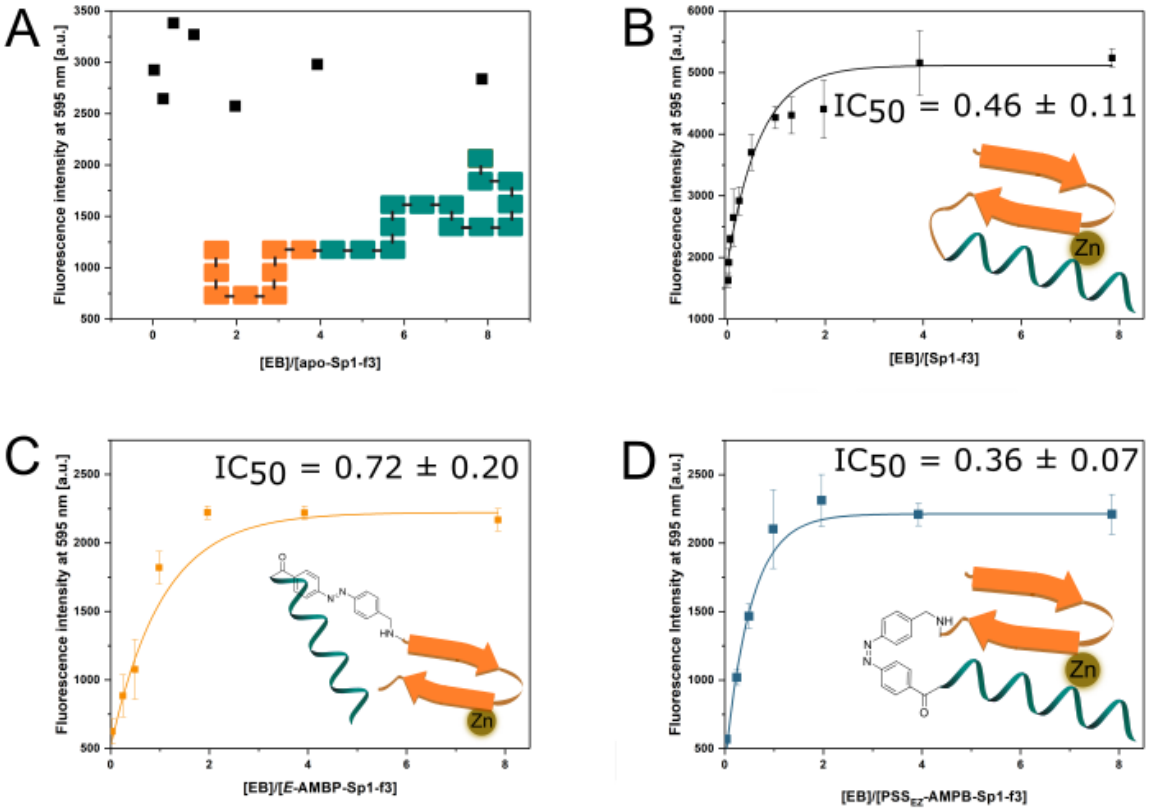

Figure 5. Fluorescence displacement assay of EB through native Zn-finger and photoswitchable Zn-fingers. Aliquots of peptide and Zn^{2+} were added to GCbox (8.8 µM, d-ATA TTA TGG GGC GGG GCC AAT ATA) intercalated with EB (0.22 mM in 10 mM TRIS buffer, NaCl 50 mM, pH 7.5, at 25°C). A) apo-Sp1-f3, B) Zn^{2+}-Sp1-f3, C) *E*-AMPB-Sp1-f3 in the presence of one eq of Zn^{2+} (with respect to the peptide) and D) AMPB-Sp1-f3 in presence of one eq of Zn^{2+} (with respect to the peptide) at the $PSS_{E\rightarrow Z}$ were investigated.

Whereas the absorbance around λ = 332 nm (λ_{max} of the *E*-isomer) stays constant, indicating no detectable *Z*-to-*E* isomerization occurring, a new transition at λ = 288 nm appears upon Zn^{2+} addition. In the next step, the sample (at $^{Zn}PSS_{E\rightarrow Z}$) was irradiated with white light to induce *Z*-to-*E* isomerization. The process was followed by UV-vis spectroscopy until no further isomerization was observed (at $^{Zn}PSS_{Z\rightarrow E}$, orange solid line in Figure 4D). The spectrum shows that the additional transition already found after addition of Zn^{2+} to the $^{Zn}PSS_{E\rightarrow Z}$, is also present at the $^{Zn}PSS_{Z\rightarrow E}$. Moreover, the CD spectrum at the at $^{Zn}PSS_{Z\rightarrow E}$ hardly shows any difference to the one at $^{Zn}PSS_{E\rightarrow Z}$ (Figure 4B) pointing to a similar tertiary structure of both photoisomers in Zn^{2+}-AMPB-Sp1-f3.

To investigate the Zn^{2+} binding towards both photoisomers of AMPB-Sp1-f3 in more detail, we determined the ion's affinity by CD titration experiments.[22] Focusing on the negative molar ellipticity at λ = 205 nm of the photochromic peptide, we followed its intensity varying the concentrations of Zn^{2+} (Figure 4C). From the obtained data, the binding constant (K_d, defined as the concentration of Zn^{2+} that leads to 50% folded peptide) of Zn^{2+} to each of the photoisomers was determined (for details, see Supporting Information). We found that *E*-AMPB-Sp1-f3 exhibits a K_d = 81 µM (1.47 eq, Figure 4C) whereas AMPB-Sp1-f3 at the $PSS_{E\rightarrow Z}$ (containing the *Z*-isomer) has a K_d = 53 µM (0.96 eq, Figure 4C). While these data do not represent a pronounced difference, they indicate that *Z*-AMPB-Sp1-f3 is a stronger zinc binder than the *E*-isomer, possibly confirming our design with the geometry in the *Z*-form favors Zn^{2+}-mediated folding of the peptide (Figure 1D).

Photocontrolled peptide-DNA binding. The binding of AMPB-Sp1-f3 and AMPB-AT-Hook to a model DNA strand was studied using fluorescence displacement assays.[31] Specifically, the peptides were titrated to a double-stranded-DNA- ethidium bromide (EB) or 4',6-diamidino-2-phenylindole (DAPI) complex, which are highly fluorescent. Thereby, a displacement of EB and DAPI by the peptides can be correlated to the decrease of the fluorescence signal as the unbound intercalators show only week fluorescence. EB is a non-specific intercalator,[32] while DAPI binds specifically to AT-rich minor groove of the DNA. Consequently, DAPI displacement should identify a potential minor groove binder.[33] The assays were performed in triplicates and the IC_{50} values (ratio of the concentration of EB or DAPI, respectively, to the concentration of the peptide that is necessary to displace half of the intercalator molecules from DNA) were calculated through exponential fitting of the obtained data (for details see Supporting Information).[32, 34]

In the case of Zn^{2+}-AMPB-Sp1-f3, the affinity of the photosensitive peptide was determined with and without irradiation and compared to the natural zinc finger, Sp1-f3 in the presence and absence of Zn^{2+}, using the model double-stranded DNA, GC-box (d-ATA TTA TGG GGC GGG GCC AAT ATA) intercalated with EB (Figure 5)[35]. For Sp1-f3, the IC_{50} was found to be 0.46±0.11 (Figure 5B), which is in the same order with values reported in

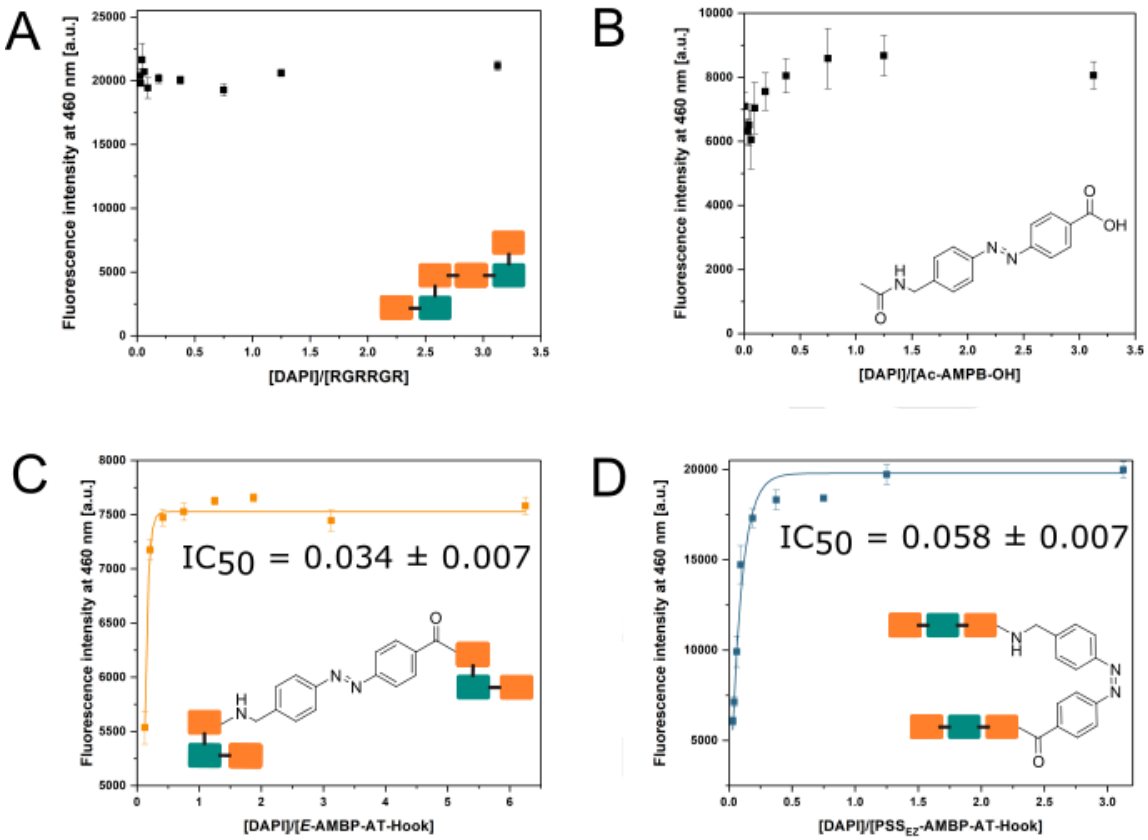

Figure 6. Fluorescence displacement assay of DAPI through RGRRGR, Ac-AMPB-OH and photoswitchable AMPB-AT-Hook. Aliquots of peptide were added to the AT-rich DNA β-hairpin sequence (0.5 μM, 5'-GCCAAAAAGCTCTCGCTTTTTGGC-3') intercalated with EB (0.2 mM in 10 mM TRIS buffer, NaCl 50 mM, pH 7.5, at 25°C). A) RGRRGR, B) Ac-AMPB-OH, C) *E*-AT-Hook and D) AMPB-AT-Hook at the $PSS_{E\rightarrow Z}$ were investigated.

literature for another DNA major-groove binder.[34] In contrast, we observed no fluorescence decrease using up to 100 eq of apo-Sp1-f3 (Figure 5A) indicating the need for Zn^{2+} to form a fully operational peptide with a well-defined tertiary structure. Moreover, in presence of Zn^{2+} AMPB-Sp1-f3 binds to DNA both at the thermal equilibrium and at $^{Zn}PSS_{E\rightarrow Z}$. Specifically, *E*-AMPB-Sp1-f3 exhibits an IC_{50} = 0.72±0.20 (Figure 5C) and, after irradiation with λ_{irrad} = 365 nm and the accompanied formation of *Z*-AMPB-Sp1-f3, the IC_{50} decreased to 0.36±0.07, a value similar to the one of natural Sp1-f3 (Figure 5D). Surprisingly, Zn^{2+}-*E*-AMPB-Sp1-f3 was found to have an even higher IC_{50} value and consequently is the stronger DNA binder. Moreover, the binding difference of approximately a factor of two for the two isomers is similar to the effect reported for the modified zinc finger of Okamoto *et al*. Despite this similar behavior; the two approaches are conceptually different: the difference in binding in our system is due to the structural perturbation of the zinc finger imposed by azobenzene, not to the interference with the DNA-binding region of the zinc finger as reported previously.[24] While a two-fold difference in binding of the two photoisomers does not yet allow for direct applications, such as *in situ* toggling of the photoswitch and real-time alteration of DNA-binding, it may pave the way to further develop valuable tool compounds.

Next, we investigated the binding affinity of both photoisomers of AMPB-AT-Hook towards the AT-rich DNA β-hairpin sequence (5'-GCCAAAAAGCTCTCGCTTTTTGGC-3') in the presence of DAPI, using Ac-AMPB-OH and the peptide RGRRGR as controls (Figure 6). DAPI was selected for its ability to bind to AT-rich regions in DNA minor grooves, similar to the AT-Hook.[5a, b] Both controls showed little to no displacement of DAPI, using up to 25 eq of RGRRGR or Ac-AMPB-OH (see Figure 6A, B). In contrast, the AMPB-AT-Hook exhibits an IC_{50} value of 0.034±0.007 in its *E*-form (Figure 6C) and of 0.058±0.007 after irradiation (containing the *Z*-isomer, Figure 6D). Consequently, the *Z*-AMPB-AT-Hook appears to be a stronger binder than the *E*-AMPB-AT-Hook, considering that the *Z*-form only contributes to 67% to the $PSS_{E\rightarrow Z}$. This is in agreement with our design, suggesting that *Z*-AMPB-AT-Hook should be the stronger binder and probably able to interact through two Hook-moieties with the same DNA strand either through binding to the minor groove or via, for instance, electrostatic interactions (*cf.* Figure 1). Similar effects were previously observed using an AT-Hook (PRGRP) attached onto a molecular motor.[26] Moreover, our designed AMPB-AT-Hook is able to act as a DNA-binder in both photoisomers whereas both controls, the peptide RGRRGR and Ac-AMPB-OH, do not appear to bind DNA. Hence, we conclude that both the aromatic and the positively charged moieties are crucial for binding of the AMPB-AT-Hook to the DNA.

Conclusions

In summary, we developed two light-responsive peptides, a photoswitchable zinc finger and an AT-Hook, that bind to the major or minor groove of a DNA α-helix, respectively. In both cases, a photoresponsive azobenzene unit was incorporated into the core of the peptide to either allow functional formation of a tertiary structure (in the case of AMPB-Sp1-f3) or provide two instead of one binding sites in the geometry of one of the photoisomers. After successful synthesis *via* SPPS and isolation of the peptides, we showed that both compounds could be photoswitched upon irradiation with light of λ = 365 nm (*E*→*Z*) or white light (*Z*→*E*). The thermal stability of the *Z*-forms was in the range of hours to days, and hence sufficient for further DNA binding studies. Both photoisomers of AMPB-Sp1-f3 were investigated regarding their ability of Zn^{2+} binding and its influence on the tertiary structure of the peptide. We found that both photoisomers were able to bind Zn^{2+}, while *Z*-isomer seemed to geometrically favor Zn^{2+} binding, presumably due to formation of a preferred tertiary structure. However, in fluorescence displacements assays, the *E*-form exhibited stronger interaction with a double stained ds-DNA. We speculate that the geometry of Zn^{2+}-AMPB-Sp1-f3 at the thermal equilibrium exposes the main binding motif, the α-helix substructure of the peptide, in an optimal way. In case of the minor-groove binder, AMPB-AT-Hook, the *Z*-isomer showed stronger interactions with the model DNA in DAPI-fluorescence displacement assays. In particular, the geometry of the *Z*-form should allow both RGR- moieties of the photosensitive peptide to interact with DNA and consequently result in stronger binding. Finally, we were able to develop photoswitchable peptides as either minor or major groove binders. In both cases, the photoisomers showed different binding modes, and hence contribute to the development of useful tools in light-controlled DNA- modulation and provide a powerful basis for applications in areas such as photodynamic gene therapy and synthetic biology.

Experimental Section

Materials and Characterization. All chemicals for synthesis were obtained from commercial sources and used as received unless stated otherwise. Solvents were reagent grade. DNA was purchased from Sigma-Aldrich. Thin-layer chromatography (TLC) was performed using commercial Kieselgel 60, F254 silica gel plates, and components were visualized with $KMnO_4$ or phosphomolybdic acid reagent. Flash chromatography was performed on silica gel (Silicycle Siliaflash P60, 40-63 m, 230-400 mesh). Drying of solutions was performed with $MgSO_4$ and solvents were removed with a rotary evaporator. Solid phase peptide synthesizer CEM Liberty, with CEM Discover microwaves was used for SPPS. RP-HPLC was carried out with Shimadzu equipment. The eluents A and B are 0.1 % TFA in acetonitrile and 0.1 % TFA in water, respectively, for all systems. Solvent ratio, gradient and flow rate are stated for each experiment individually. For analytical RP-HPLC, an XTerra C18 3.0x150mm column (Waters) was used, for semi-preparative RP-HPLC, an XTerra Prep C18 7.8x150mm column (Waters), and for UPLC XTerra Prep MS C6 10 µm was used. UV/Vis absorption spectra were recorded on an Agilent 8453 UV-Visible Spectrophotometer using spectroscopic grade solvents (Uvasol by Merck). CD spectra were recorded on JASCO J815. Irradiation experiments were performed with a spectroline ENB-280C/FE UV lamp (312 nm) or an OSL1-EC from ThorLabs (white light). Chemical shifts for NMR measurements are reported relative to an internal standard (residual solvent peaks). The following abbreviations are used to indicate signal multiplicity: s, singlet; d, doublet; t, triplet; q, quartet; m, multiplet; br s, broad signal. HRMS (ESI) spectra were obtained on a Thermo scientific LTQ Orbitrap XL. MALDI spectra were obtained on a MALDI/TOFTOF 4800 by AB Sciex; the analysis was done in positive mode using the matrix *alpha*-cyano-hydroxycinnamic acid. Melting points were recorded using a Buchi melting point B-545 apparatus.

General procedure for oligopeptide synthesis *via* SPPS. All peptides were synthesized on a 0.1 mmol scale by standard Fmoc strategy for SPPS using a peptide synthesizer and Sieber resin (0.69 mmol/g). Fmoc-Ala-OH, Fmoc Phe-OH, Fmoc-Cys(Trt) Fmoc-Lys(Trt)-OH, Fmoc-Pro-OH, Fmoc-Glu(O-2-PhiPr)-OH, Foc Arg(Pbf)-OH, Foc-Met-OH, Fmoc-Ser(Trt)-OH, Fmoc-Asp(O-2-PhiPr)-OH, Fmoc-His(Trt)-OH, Fmoc-Leu-OH, Fmoc-Ile-OH, Fmoc-Thr(Trt)-OH, Fmoc-Gln(Trt)-OH, Fmoc-Asn(Trt)-OH were used. The coupling steps were performed with 5 eq Fmoc-protected amino acid, 5 eq HBTU and 10 eq DIPEA (2 x 45 min). The Fmoc-deprotection step was performed with 20% piperidine in DMF (1 x 30 min). The acetylation step was performed with 10 eq. Ac_2O, 0.1 eq. HOBt and 10 eq. DIPEA. Cleavage from the resin was performed at rt for 75 min with TFA:water (95:5) under a nitrogen atmosphere.

Synthesis of AMPB-Sp1-f3. The peptide was synthesized following the general procedure for SPPS. The crude peptide was purified by RP-HPLC on C18 semi-preparative column (method: 3 min at 5% B in A and then linear gradient of 1.54% of eluent A per min; flow rate of 0.5 $mLmin^{-1}$). Purity (220 nm): 76%. R_t: 17.8 min (*E*-isomer). MADLI-TOF: calcd. 3806 [M^+]; found: 3803 [M^+].

Synthesis of Sp1-f3. The peptide was synthesized following the general procedure for SPPS. The crude peptide was purified by RP-HPLC on C18 semi-preparative column (HPLC method: 3 min 10% B in A, then linear gradient to 90% B in A (in 58 min), then 95% B in A for 2 min; flow rate of 0.5 $mLmin^{-1}$). Purity: 80% (215 nm). R_t: 28.3 min (*E*-isomer). MADLI-TOF: calcd. 3524 [M^+]; found: 3524 [M^+].

Synthesis of AMPB-AT-Hook. The synthesis was performed as described in general procedure. Fmoc-AMPB-OH (40 mg, 84 mmol) was used in the coupling reaction. The UPLC spectrum of crude material and the HPLC traces of pure fractions are reported in Figure S3 a,b,c, respectively. AMPB-AT-Hook was obtained in 97 % yield (80 mg). Purity: 81% (220 nm). R_t: 14.70 min. HRMS m/z calcd. for $C_{42}H_{68}N_{22}O_7$ [M+H]$^+$: 992.5641; found: 992.5639 [M+H]$^+$.

Spectroscopic experiments, CD measurements and further details regarding the DNA binding studies are available in the Supporting Information.

Acknowledgements

We gratefully acknowledge generous support from NanoNed, The Netherlands Organization for Scientific Research (NOW-CW, Top grant to B.L.F. and NWO VIDI grant no. 723.014.001 for W.S.), the Royal Netherlands Academy of Arts and Sciences (KNAW), the Ministry of Education, Culture and Science (Gravitation program 024.001.035), and the European Research Council (Advanced Investigator Grant no. 694345 to B.L.F.). We thank James Z. Butler for the support.

Keywords: DNA binding • photoswitching • zinc finger • AT-Hook • photocontrol • peptides

[1] a) K. E. Van Holde and I. Isenberg, *Acc. Chem. Res.* **1975**, *8*, 327-335; b) a. S C R Elgin and H. Weintraub, *Annu. Rev. Biochem.* **1975**, *44*, 725-778; c) A. B. Georges, B. A. Benayoun, S. Caburet and R. A. Veitia, *FASEB J.* **2010**, *24*, 346-356; d) N. M. Luscombe, S. E. Austin, H. M. Berman and J. M. Thornton, *Genome Biology* **2000**, *1*, reviews001.001-001.37; e) M. E. Vázquez, A. M. Caamaño, J. L. Mascareñas, *Chem. Soc. Rev.* **2003**, *32*, 338-349; f) T. Morii, *Bull. Chem. Soc. Jpn.* **2017**, *90*, 1309-1317.

[2] a) K. Chockalingam, M. Blenner and S. Banta, *Protein Eng. Des. Sel.* **2007**, *20*, 155-161; b) D. W. P. M. Löwik, E. H. P. Leunissen, M. van den Heuvel, M. B. Hansen and J. C. M. van Hest, *Chem. Soc. Rev.* **2010**, *39*, 3394-3412; c) R. J. Mart, R. D. Osborne, M. M. Stevens and R. V. Ulijn,

Soft Matter. **2006**, *2*, 822-835; d) S. Learte-Aymamí, N. Curado, J. Rodríguez, M. E. Vázquez, J. L. Mascareñas, *J. Am. Chem. Soc.* **2017**, 139, 16188-16193; e) J. Rodríguez, J. Mosquera, M. E. Vázquez, J. L. Mascareñas, *Chem. Eur. J.* **2016**, *22*, 13474-13477.

[3] a) S. Wong, M. S. Shim and Y. J. Kwon, *J. Mater. Chem. B* **2014**, *2*, 595-615; b) Y. Liu, Y. Yang, C. Wang and X. Zhao, *Nanoscale* **2013**, *5*, 6413-6421.

[4] a) W. Szymański, J. M. Beierle, H. A. V. Kistemaker, W. A. Velema and B. L. Feringa, *Chem. Rev.* **2013**, *113*, 6114-6178; b) C. Renner and L. Moroder, *ChemBioChem* **2006**, *7*, 868-878; c) A. S. Lubbe, W. Szymanski and B. L. Feringa, *Chem. Soc. Rev.* **2017**, *46*, 1052-1079; d) P. Klán, T. Šolomek, C. G. Bochet, A. Blanc, R. Givens, M. Rubina, V. Popik, A. Kostikov and J. Wirz, *Chem. Rev.* **2013**, *113*, 119-191; e) C. Brieke, F. Rohrbach, A. Gottschalk, G. Mayer and A. Heckel, *Angew. Chem. Int. Ed.* **2012**, *51*, 8446-8476; f) E. Pazos, J. Mosquera, M. E. Vázquez, J. L. Mascareñas, *ChemBioChem* **2011**, *12*, 1958-1973; g) G. A. Bullen, J. H. R. Tucker, A. F. A. Peacock, *Chem. Commun.* **2015**, *51*, 8130-8133; h) A. Jiménez-Balsa, E. Pazos, B. Martínez-Albardonedo, J. L. Mascareñas, M. E. Vázquez, *Angew. Chem. Int. Ed.* **2012**, *51*, 8825-8829; i) M. I. Sánchez, J. Martínez-Costas, F. Gonzalez, M. A. Bermudez, M. E. Vázquez, J. L. Mascareñas, *ACS Chem. Biol.* **2012**, *7*, 1276-1280.

[5] a) A. A. Beharry and G. A. Woolley, *Chem. Soc. Rev.* **2011**, *40*, 4422-4437; b) C. Poloni, W. Szymański, L. Hou, W. R. Browne and B. L. Feringa, *Chem. Eur. J.* **2014**, *20*, 946-951; c) C. Knie, M. Utecht, F. Zhao, H. Kulla, S. Kovalenko, A. M. Brouwer, P. Saalfrank, S. Hecht and D. Bléger, *Chem. Eur. J.* **2014**, *20*, 16492-16501; d) M. A. Kienzler, A. Reiner, E. Trautman, S. Yoo, D. Trauner and E. Y. Isacoff, *J. Am. Chem. Soc.* **2013**, *135*, 17683-17686; e) L. Albert, J. Xu, R. Wan, V. Srinivasan, Y. Doub and O. Vázquez, *Chem. Sci.* **2017**, *8*, 4612-4618.

[6] a) M. Singer and A. Jäschke, *J. Am. Chem. Soc.* **2010**, *132*, 8372-8377; b) C. Hana and J. Andres, *Angew. Chem. Int. Ed.* **2013**, *52*, 3186-3190.

[7] a) R. L. Letsinger and T. Wu, *J. Am. Chem. Soc.* **1995**, *117*, 7323-7328; b) F. D. Lewis and X. Liu, *J. Am. Chem. Soc.* **1999**, *121*, 11928-11929; c) F. D. Lewis, Y. Wu and X. Liu, *J. Am. Chem. Soc.* **2002**, *124*, 12165-12173.

[8] a) Y. Kamiya and H. Asanuma, *Acc. Chem. Res.* **2014**, *47*, 1663-1672; b) S. Samanta, A. Babalhavaeji, M.-x. Dong and G. A. Woolley, *Angew. Chem.* **2013**, *125*, 14377-14380; c) S. Samanta, A. A. Beharry, O. Sadovski, T. M. McCormick, A. Babalhavaeji, V. Tropepe and G. A. Woolley, *J. Am. Chem. Soc.* **2013**, *135*, 9777-9784.

[9] a) G. Gauglitz, *J. Photochem.* **1976**, *5*, 41-47; b) G. Gauglitz and S. Hubig, *J. Photochem.* **1981**, *15*, 255-257.

[10] J. Li, X. Wang and X. Liang, *Chem. Asian J.* **2014**, *9*, 3344-3358.

[11] R. Gu, J. Lamas, S. K. Rastogi, X. Li, W. Brittain and S. Zauscher, *Colloids Surf.. B* **2015**, *135*, 126-132.

[12] S. Schimka, S. Santer, N. M. Mujkić-Ninnemann, D. Bléger, L. Hartmann, M. Wehle, R. Lipowsky and M. Santer, *Biomacromolecules* **2016**, *17*, 1959-1968.

[13] F. Ciardelli, S. Bronco, P. Pieroni, A. Pucci (2011). Photo-switchable Polypeptides. In: Molecular Switches (eds. B. L. Feringa, W. R. Browne), 321–360, 2nd ed.; Wiley-VCH: Weinheim.

[14] a) M. Suzuki, N. Yagi and M. Gerstein, *Protein Eng. Des. Sel.* **1995**, *8*, 329-338; b) C. Murre, P. S. McCaw, H. Vaessin, M. Caudy, L. Y. Jan, Y. N. Jan, C. V. Cabrera, J. N. Buskin, S. D. Hauschka, A. B. Lassar, H. Weintraub and D. Baltimore, *Cell* **1989**, *58*, 537-544.

[15] a) E. Blackwood and R. Eisenman, *Science* **1991**, *251*, 1211-1217; b) W. Landschulz, P. Johnson and S. McKnight, *Science* **1988**, *240*, 1759-1764; c) J. R. Kumita, D. G. Flint, G. A. Woolley and O. S. Smart, *Faraday Discuss.* **2002**, *122*, 89-103; d) A. M. Caamaño, M. E. Vázquez, J. Martínez-Costas, L. Castedo and J. L. Mascareñas, *Angew. Chem. Int. Ed.* **2000**, *39*, 3104-3107; e) G. A. Woolley, A. S. I. Jaikaran, M. Berezovski, J. P. Calarco, S. N. Krylov, O. S. Smart and J. R. Kumita, *Biochemistry* **2006**, *45*, 6075-6084.

[16] a) G. M. Church, J. L. Sussman and S. H. Kim, *P. Natl. A. Sci.* **1977**, *74*, 1458-1462; b) W. S. Somers and S. E. V. Phillips, *Nature* **1992**, *359*, 387-393.

[17] a) A. A. Beharry and G. A. Woolley, *Neuromethods* **2011**, *55*, 171-184; b) G. Merutka, W. Shalongo and E. Stellwagen, *Biochemistry* **1991**, *30*, 4245-4248; c) D. C. Burns, F. Zhang and G. A. Woolley, *Nat. Protoc.* **2007**, *2*, 251-258; d) A. M. Ali and G. A. Woolley, *Org. Biomol. Chem.* **2013**, *11*, 5325-5331; e) M. Blanco-Lomas, S. Samanta, P. J. Campos, G. A. Woolley and D. Sampedro, *J. Am. Chem. Soc.* **2012**, *134*, 6960-6963; f) S. Samanta, C. Qin, A. J. Lough and G. A. Woolley, *Angew. Chem. Int. Ed.* **2012**, *51*, 6452-6455; g) L. Nevola, A. Martín-Quirós, K. Eckelt, N. Camarero, S. Tosi, A. Llobet, E. Giralt and P. Gorostiza, *Angew. Chem. Int. Ed*. **2013**, *52*: 7704-7708; h) G. A. Woolley, *Acc. Chem. Res.* **2005**, *38*, 486-493.

[18] a) S.-L. Dong, M. Löweneck, T. E. Schrader, W. J. Schreier, W. Zinth, L. Moroder and C. Renner, *Chem. Eur. J.* **2006**, *12*, 1114-1120; b) A. Aemissegger, V. Kräutler, W. F. van Gunsteren and D. Hilvert, *J. Am. Chem. Soc.* **2005**, *127*, 2929-2936; c) A. A. Deeg, M. S. Rampp, A. Popp, B. M. Pilles, T. E. Schrader , L. Moroder, K. Hauser and W. Zinth, *Chem. Eur. J.* **2014**, *20*, 694-703; d) T. Podewin, M. S. Rampp, I. Turkanovic, K. L. Karaghiosoff, W. Zinth and A. Hoffmann-Röder, *Chem. Commun.* **2015**, *51*, 4001-4004.

[19] a) D. E. Wemmer and P. B. Dervan, *Curr. Opin. Struct. Biol.* **1997**, *7*, 355-361; b) E. Pazos, J. Mosquera, M. E. Vázquez and J. L. Mascareñas, *ChemBioChem* **2011**, *12*, 1958-1973.

[20] a) S. N. Shah, L. Cope, W. Poh, A. Belton, S. Roy, C. C. Talbot, S. Sukumar, D. L. Huso and L. M. S. Resar, *PLoS ONE* **2013**, *8*, e63419; b) A. Belton, A. Gabrovsky, Y. K. Bae, R. Reeves, C. Iacobuzio-Donahue, D. L. Huso and L. M. S. Resar, *PLoS ONE* **2012**, *7*, e30034; c) R. Hock, T. Furusawa, T. Ueda and M. Bustin, *Trends Cell Biol.* **2007**, *17*, 72-79; d) R. Reeves, *Gene* **2001**, *277*, 63-81.

[21] a) A. Klug, *Annu. Rev. Biochem.* **2010**, *79*, 213-231; b) S. A. Wolfe, L. N. and and C. O. Pabo, *Annu. Rev. Bioph. Biom.* **2000**, *29*, 183-212.

[22] a) A. D. Frankel, J. M. Berg and C. O. Pabo, *P. Natl. A. Sci. USA* **1987**, *84*, 4841-4845; b) J. Miller, A. D. McLachlan and A. Klug, *EMBO J.* **1985**, *4*, 1609-1614.

[23] C. Chou and A. Deiters, *Angew. Chem. Int. Ed.* **2011**, *50*, 6839-6842.

[24] A. Nomura and A. Okamoto, *Chem. Commun.* **2009**, 1906-1908.

[25] a) R. Behrendt, M. Schenk, H.-J. Musiol and L. Moroder, *J. Pept. Sci.* **1999**, *5*, 519-529; b) L. Ulysse and J. Chmielewski, *Bioorg. Med. Chem. Lett.* **1994**, *4*, 2145-2146.

[26] F. Nagatsugi, Y. Takahashi, M. Kobayashi, S. Kuwahara, S. Kusano, T. Chikuni, S. Hagihara and N. Harada, *Mol. Biosyst.* **2013**, *9*, 969-973.

[27] a) V. A. Narayan, R. W. Kriwacki and J. P. Caradonna, *J. Biol. Chem.* **1997**, *272*, 7801-7809; b) M. Yokono, N. Saegusa, K. Matsushita and Y. Sugiura, *Biochemistry* **1998**, *37*, 6824-6832; c) S. Oka, Y. Shiraishi, T. Yoshida, T. Ohkubo, Y. Sugiura and Y. Kobayashi, *Biochemistry* **2004**, *43*, 16027-16035; d) J. T. Kadonaga, K. A. Jones and R. Tjian, *Trends Biochem. Sci.* **1986**, *11*, 20-23.

[28] B. Priewisch and K. Rück-Braun, *J. Org. Chem.* **2005**, *70*, 2350-2352.

[29] a) G. B. Field and R. L. Noble, *Int. J. Pept. Protein Res.* **1990**, *35*, 161-214; b) R. B. Merrifield, *J. Am. Chem. Soc.* **1963**, *85*, 2149-2154; c) R. B. Merrifield, *J. Am. Chem. Soc.* **1964**, *86*, 304-305; d) E. Atherton and R. C. Sheppard (1989). *Solid phase peptide synthesis: a practical approach*. IRL Press at Oxford University Press, Oxford, England.

[30] M. Löweneck, A. G. Milbradt, C. Root, H. Satzger, W. Zinth, L. Moroder and C. Renner, *Biophys. J.* **2006**, *90*, 2099-2108.

[31] W. C. Tse and D. L. Boger, *Acc. Chem. Res.* **2004**, *37*, 61-69.

[32] a) M. J. Waring, *J. Mol. Biol.* **1965**, *13*, 269-282; b) B. F. Cain, B. C. Baguley and W. A. Denny, *J. Med. Chem.* **1978**, *21*, 658-668; c) D. L. Boger, B. E. Fink and M. P. Hedrick, *J. Am. Chem. Soc.* **2000**, *122*, 6382-6394; d) V. A. Izumrudov, M. V. Zhiryakova and A. A. Goulko, *Langmuir* **2002**, *18*, 10348-10356.

[33] Y. Chai, M. Munde, A. Kumar, L. Mickelson, S. Lin, N. H. Campbell, M. Banerjee, S. Akay, Z. Liu, A. A. Farahat, R. Nhili, S. Depauw, M.-H. David-Cordonnier, S. Neidle, W. D. Wilson and D. W. Boykin, *Int. J. Pept. Prot. Res.* **2014**, *15*, 68-79.

[34] Y.-H. Shim, P. B. Arimondo, A. Laigle, A. Garbesi and S. Lavielle, *Org. Biomol. Chem.* **2004**, *2*, 915-921.

[35] D. Gidoni, J. Kadonaga, H. Barrera-Saldana, K. Takahashi, P. Chambon and R. Tjian, *Science* **1985**, *230*, 511-517.

Entry for the Table of Contents

Layout 1:

FULL PAPER

Sequence-specific small peptide-DNA major and minor groove interactions can be controlled by irradiation. Specifically, photoswitchable azobenzene moieties were implemented in the peptide backbone or turn region of transcriptionally active peptides. DNA binding affinity was affected by photochemical isomerization, which provides promising tools for DNA modulation.

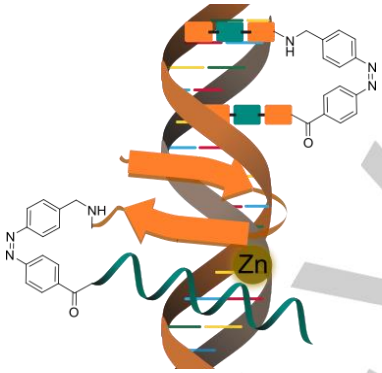

Gosia M. Murawska, Claudia Poloni, Nadja A. Simeth, Wiktor Szymanski* and Ben L. Feringa*

Page No. – P6age No.

Comparative study of photoswitchable zinc finger domain and AT-hook motif for light-controlled peptide-DNA binding

Layout 2:

FULL PAPER

((Insert TOC Graphic here; max. width: 11.5 cm; max. height: 2.5 cm))

*Author(s), Corresponding Author(s)**

Page No. – Page No.

Title

Text for Table of Contents